AIE-active bis-cyanostilbene-based organogels for quantitative fluorescence sensing of CO_2 based on molecular recognition principles†

Yao Ma, [a] Massimo Cametti,*[b] Zoran Džolić [c] and Shimei Jiang*[a]

Carbon dioxide is a major greenhouse gas, probably responsible for climate change, and a safety concern for workers under specific conditions. Simple and effective means for its detection are thus highly desirable. Herein, the aggregation-induced emissive bis-cyanostilbene derivative **1** was used to develop two sensor systems based on (i) dispersed gel aggregates and (ii) solid supported xerogels for the optical detection of CO_2 gas. In the presence of diethylamine, CO_2 is transformed into a carbamate ionic liquid (CIL), which binds to **1** acting as an anion receptor. The formation of such a host–guest adduct alters the aggregation state of the system and consequently its fluorescence, which thus responds to CO_2 concentration. While the gel aggregate sensing system responds to CO_2 *via* fluorescence quenching, the xerogel sensor system works in a dual mode, *i.e.*, by both fluorescence quenching and modulation, reaching very high sensitivity and a low detection limit (4.5 ppm). The sensing behavior of **1** (gel aggregate and xerogel systems) towards CO_2 gas was studied in detail by solid state fluorescence and solution ^{1}H-NMR spectroscopies.

Introduction

In the last few years, concerns over the environmental effects of carbon dioxide, CO_2, in terms of global warming, have generated widespread discussion.[1] Moreover, CO_2 represents a major health and safety concern for workers operating in confined spaces.[2] Undetectable by the human senses, CO_2 has indeed been reported to cause health problems at concentrations as high as 3000 ppm after long exposures (average atmospheric CO_2 concentration is *ca.* 400 ppm). However, at higher concentrations, it can lead to several physiological dysfunctions and, eventually, to irreversible damage.[3]

Several methods are currently used for the detection of CO_2,[4] the most common of which is based on infrared (IR) spectroscopy. Indeed, most commercially available CO_2 sensors are IR detectors. Other methods also comprise potentiometric and gas-chromatographic techniques. However, all these conventional methods are limited by either high costs or low portability or insufficient selectivity, and often by the need for complex and time-consuming procedures. Hence, it is of great importance to develop a sensitive method for the *in situ* detection and quantitative determination of CO_2 gas in real-world environments that could be carried out rapidly and with portable instrumentation.

Recently, absorbance and fluorescence techniques have drawn attention precisely in this regard, as they could represent an alternative route for CO_2 detection, featuring high selectivity and sensitivity, being practically convenient, of low cost and capable of a rapid real-time response.[5] In particular, the aggregation induced emission (AIE) phenomenon, where the fluorophore exhibits weak fluorescence in solution but is highly emissive in the aggregated state, is quite promising for the development of novel sensing systems, especially when supramolecular aggregation/disaggregation processes are relevant.[6]

There exist two main strategies for the design of CO_2 sensor systems based on an optical response (either absorption or emission), and both rely on the electrophilic nature of CO_2, which can react with good nucleophiles, such as aliphatic amines, to form carbamates, or with other nucleophilic species (N-heterocyclic carbenes, *etc.*). The sensing mechanism is either due to a direct modification of the sensor molecule upon reaction with CO_2,[7] or due to a CO_2 induced physico-chemical change of the medium (polarity, viscosity, pH, *etc.*), which in turn influences

[a] *State Key Laboratory of Supramolecular Structure and Materials, College of Chemistry, Jilin University, 2699 Qianjin Avenue, Changchun, 130012, P. R. China. E-mail: smjiang@jlu.edu.cn; Fax: +86-431-85193421; Tel: +86-431-85168474*

[b] *Department of Chemistry, Materials and Chemical Engineering "Giulio Natta", Politecnico di Milano, Via L. Mancinelli 7, 20131 Milano, Italy. E-mail: massimo.cametti@polimi.it*

[c] *Ruđer Bošković Institute, Bijenička cesta 54, 10000 Zagreb, Croatia*

† Electronic supplementary information (ESI) available: Detailed synthetic procedures and characterization data, NMR spectra, FT-IR spectra, DLS analysis, UV/Vis and fluorescence spectra. See DOI: 10.1039/c8tc01190g

This is the accepted version of Ma Y., Cametti M., Džolić Z., Jiang S., "AIE-active bis-cyanostilbene-based organogels for quantitative fluorescence sensing of CO2 based on molecular recognition principles", Journal of Material Chemistry C (2018), 6, 9232-9237.
The final publication is available at https://doi.org/10.1039/C8TC01190G

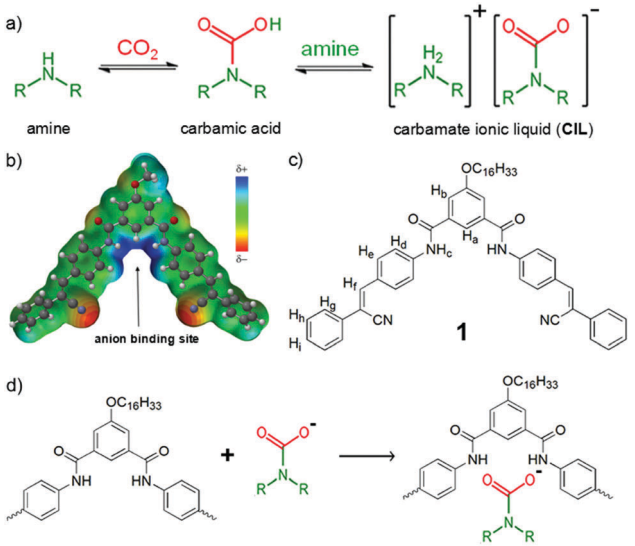

Scheme 1 (a) Generic reaction scheme for the formation of a carbamate ionic liquid (CIL) by CO_2 and an aliphatic amine R_2NH; (b) electrostatic potential map for the methoxyl substituted derivative calculated at the DFT B3LYP (6-31G**) level of theory; (c) molecular formula of gelator **1**; (d) proposed host–guest complex formation between **1** and the CIL counter anion.

the absorption/emission properties of the sensor dissolved in it.[8] In the former case, the reaction with CO_2 is often aided by a previous deprotonation step, while in the latter case, the modulation of the medium characteristics by CO_2 is most commonly due to the formation of a carbamate ionic liquid (CIL) (Scheme 1a).

Low-molecular-weight organic gelators (LMWOGs) have been widely investigated for their properties from a fundamental point of view, especially regarding the mechanism of self-assembly and the resulting gel morphology,[9] but also for their potential in a wide range of technological applications.[10] The design of novel soft materials capable of responding to specific external stimuli and translating them into a macroscopic response, possibly controllable and reversible, represents indeed one of the most fascinating and challenging goals of current research in supramolecular chemistry. Recently, we have successfully developed novel responsive AIE organogel systems based on a set of LMWOGs featuring bis-cyanostilbene moieties. Gelation readily occurred in various organic solvents,[11] and the gels exhibited a specific response towards trifluoroacetic acid.[12]

These bis-cyanostilbene derivatives showed interesting anion-binding properties derived from the two converging amidic NHs in the isophthlamidic central moiety, a classic anion binding site. We reasoned that the *in situ* formed CIL anion's carboxylate group could interact with this class of gelator molecules in the gel phase (see Scheme 1b for the electrostatic potential map that evidences the more Lewis acidic region in blue color), thus altering the gelator aggregation state and inducing detectable fluorescence changes. Such changes would thus be dependent on CO_2 concentration and be suitable for use in sensing. The combination of a simple aliphatic amine that could form a CIL in the presence of CO_2 and the appropriate bis-cyanostilbene derivative could indeed represent a viable sensing system for CO_2 gas.

In this work, we have tested this novel strategy for CO_2 sensing based on molecular recognition principles. Herein, we report on two fluorescent CO_2 gas sensor systems made of gel aggregates and xerogel films of **1** (Scheme 1c), respectively. At variance with other systems previously reported,[7,8] CO_2 sensing is here achieved through the formation of a host–guest complex between the gelator molecules and the CIL's anion, which is obtained *in situ* by reaction of CO_2 with aliphatic diethylamine (DEA) (Scheme 1d). While the gel aggregate system of **1** responds to CO_2, in the presence of excess DEA, by emission quenching with moderate sensitivity (detection limit of 908 ppm), most notably, the xerogel film system of **1** represents a significant advancement. Indeed, it allows for the detection of CO_2 by a dual mode, *i.e.*, by both fluorescence quenching and modulation, reaching a very high sensitivity and a low detection limit, as low as 4.5 ppm. The above mentioned xerogel system also possesses all the benefits of solid state sensors, such as increased stability and portability, for use in potential real-world applications.

Results and discussion

Bis-cyanostilbene derivative **1** was synthesized by adapting a previously reported procedure[12] and fully characterized (see ESI†). Indeed, **1** has AIE properties. As shown in Fig. S3 (ESI†), **1** is almost non-emissive in tetrahydrofuran (THF) solution, while the emission intensity increases dramatically upon increasing the water molar fraction (χ_w). In addition, a significant red shift of the emission occurs ($\Delta\lambda$ = 44 nm). As far as UV-Vis absorption is concerned, the UV-Vis absorption band of **1** is red-shifted upon increasing the water molar fraction (χ_w) along with a gradual decrease in the intensity. This clearly indicates that the environment can affect the aggregation of **1**, and these data are consistent with the cyanostilbene moieties stacking together in J-type arrays.[13]

Compound **1** acts as a good gelator in many aromatic solvents (Table S1, ESI†), with the critical gelation concentration, cgc, as low as 3.3 wt% in the case of toluene, and often lower than 4 wt%. Gelation occurs due to a combination of several different intermolecular interactions, with a major contribution from aromatic stacking which, in the aggregated state, limits non-emissive relaxation pathways. As depicted in Fig. 1, the toluene gel of **1** is strongly fluorescent (λ_{em} = 465 nm; λ_{ex} = 365 nm), while its solution state, obtained by increasing temperature, is weakly fluorescent featuring a slightly blue shifted maximum (λ_{em} = 445 nm; λ_{ex} = 365 nm). This confirms the decreased co-planarization of the phenyl groups, along with a more twisted molecular conformation of **1** in solution, due to the loss of the π–π interactions.[14] The hydrogen bonding (HB) interactions were measured by temperature-dependent FT-IR (Fig. S4, ESI†). As the temperature rose, the N–H stretching band at 3260 cm^{-1} and the C═O stretching band at 1663 cm^{-1} both slowly shifted to a higher frequency, indicating a non-negligible role of HB in the gel formation.

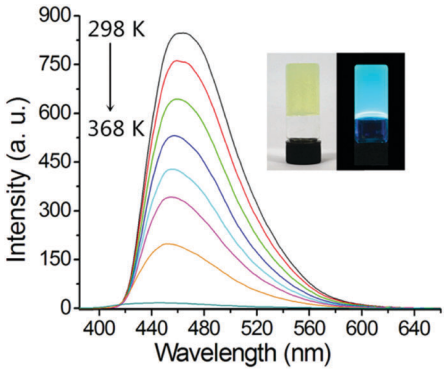

Fig. 1 Temperature-dependent fluorescent spectra of the toluene gel of **1** (λ_{ex} = 365 nm). Inset: Photographs of the gel under ambient and UV light.

As noted before, the amidic NH arrangement makes **1** a potentially good HB receptor for anions. As far as the gel response to the addition of anionic substrates (as their TBA salts) is concerned, we found that among the common anions, the addition of chloride, bromide and acetate produces a gel-to-solution transition of the toluene gel of **1**. Notably, CIL also induces such a gel disruption (Fig. 2a).[15] This moderate anion selectivity was also tested in solution, in order to confirm the validity of previous indications of the anion binding ability of compounds similar to **1** and also to quantitatively evaluate its affinity for anions.

^{1}H-NMR titrations of **1** with (TBA)X salts (X = Cl, Br, I, AcO, NO_3, PF_6 and ClO_4) and CIL were thus conducted in DMSO-d_6 : D_2O 98 : 2.[16]

The family of spectra for the titration of **1** with (TBA)OAc is shown in Fig. 2b.[17] The addition of increasing amounts of the anion induces marked downfield shifts of the amidic NHs (Hc) and of aromatic Ha, while smaller changes can be observed for the Hd, and He and Hf signals, which, initially overlapping, can then be discriminated at a higher anion concentration.

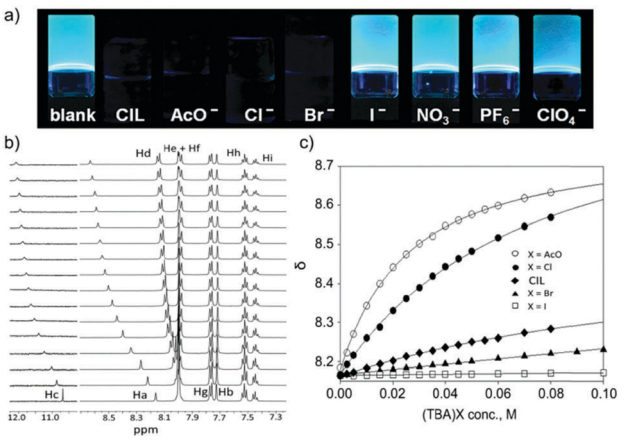

Fig. 2 (a) Photographs of the gel (10 mg of 1 in 2.9 mL of toluene) before and after addition of the CIL and anions under UV light; (b) chemical shift variations of the signals of **1** (5×10^{-3} M) upon the addition of increasing amounts of (TBA)OAc (from bottom to top, 0–16 eq.) in DMSO-d_6 : D_2O 98 : 2 at 300 K. (c) Plot of the Ha chemical shift variations of **1** *vs.* (TBA)X (X = Cl, Br, I, AcO) and CIL concentration. Lines represent best fit curves.

A plot of the chemical shift variations for the Ha signal upon addition of (TBA)X (X = Cl, Br, I, AcO) and CIL is shown in Fig. 2c. Data were fitted by a non-linear least square to a 1 : 1 binding isotherm to afford the apparent association constant K (M^{-1}). Acetate is the anion bound best by **1** under the experimental conditions used with K equal to *ca.* 50 M^{-1}, while Cl^- shows a K equal to *ca.* 15. Br^- and I^- were bound very weakly (K of *ca.* 2 for Br^- and < 1 for I^-). As far as the CIL is concerned, the observed K is *ca.* 7 M^{-1}. No detectable changes in the chemical shifts of **1** were observed by adding (TBA)NO_3 or (TBA)PF_6 or (TBA)ClO_4. These data qualitatively follow the trend of gel stability mentioned before, with the notable exception of Br^- which, despite the very weak binding in DMSO–water solution, is capable of efficiently disrupting the toluene gel. Additional evidence of anion–gelator interactions can also be observed by recording the ^{1}H-NMR spectra of the toluene-d_8 gel of **1** in the presence of varying amounts of (TBA)Cl and CIL (see Fig. S6, ESI†).

The data presented so far collectively show that the fluorescent gel of **1** can be selectively turned into a non-emissive solution by the addition of anions such a AcO^-, Cl^- and the carbamate ion of CIL, and that the underlying mechanism of response is represented by the formation of a HB complex between the given anion and **1**. As the CIL can be formed *in situ* by bubbling CO_2 into a solution containing simple aliphatic amines (for example, DEA, used in this work, see Fig. S7, ESI†), the fluorescent response of **1**-gel to CIL could in turn be a way to sense CO_2 gas. Having this idea in mind, we first analysed the effect of DEA on **1** and the toluene gel of **1**. In solution, no apparent specific interaction can be detected by ^{1}H-NMR spectroscopy (see Fig. S8, ESI†). Interestingly, we found that DEA is able instead to partially disassemble the bulk gel. However, depending on the quantity of DEA used (%v/v), the dimension of gel aggregates can be modulated and fluorescence partially maintained (see Fig. S9a and b, ESI†).

In order to use a gel system for gas sensing purposes, a large surface area is a prerequisite and thus bulk gels are not optimal. A compromise between initial emission intensity, sensitivity and response time needed to be found. In our experimental setup, the original gel is thus turned into a pseudo-homogeneous flowable dispersion of gel-aggregates (Fig. 3a) by using 16.7% DEA (5 : 1 v/v). Under these conditions, dynamic light scattering (DLS) analysis shows an average particle dimension of *ca.* 4 μm (Fig. S10, ESI†). The initial emission of the gel-aggregates appears at 455 nm (Fig. 3b). Known volumes of CO_2 were then gradually added into the sensor sample and the fluorescence was recorded. As expected, the fluorescence intensity descended very steeply, and after adding *ca.* 15 equivalents (with respect to the gelator) of CO_2, the mixture turned into a non-fluorescent solution, as depicted in Fig. 3b and c. Over the 0–9 mM range, a linear calibration line (R = 0.9986) was attained and the detection limit was calculated to be 908 ppm (Fig. S11, ESI†). The ^{1}H-NMR spectra of gel aggregates after the addition of different volumes of CO_2 (Fig. S12, ESI†) are fully consistent with the formation of a complex between **1** and the carbamate ion as the origin of the observed fluorescence quenching. Thus, the **1**-gel/DEA system

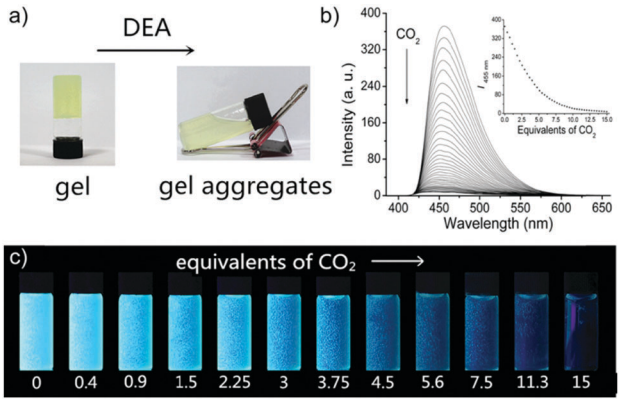

Fig. 3 (a) Photos of the gel (10 mg of **1** in 2.9 mL toluene) and the gel-aggregates (gel/DEA, 5 *vs.* 1 v/v); (b) fluorescent spectra of the gel-aggregates upon bubbling increasing amounts of CO_2 (λ_{ex} = 365 nm). Inset: Plot of the intensity at 455 nm *versus* CO_2 concentration (expressed as equivalents to **1**); (c) photos of the gel-aggregates with different CO_2 concentration (irradiated under 365 nm light).

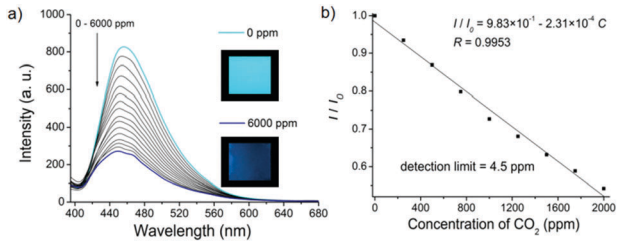

Fig. 4 (a) Fluorescent spectra of the xerogel film exposed to different concentrations of CO_2 (from 0 to 6000 ppm) in the presence of DEA vapor; inset: images of the starting and final xerogels under UV illumination; (b) plot of the normalized fluorescence intensity at 460 nm *versus* different concentrations of CO_2 in the 0–2000 ppm range (I: I_{460nm}, C: concentration of CO_2).

can indeed act as a fluorescent sensor for CO_2 gas with the advantage of a high read-out signal contrast (going from a strong blue emission to almost complete disappearance of the fluorescence). On the other hand, the sensitivity is low and the system is impractical, as storing, carrying and handling solutions can be problematic for real-world applications (see Fig. S9c–f in ESI† for tests with other amines).

In order to improve the characteristics of our sensor system, we set out to investigate the properties of xerogel films made from the **1**-gel. In general, xerogel films are easily fabricated from organogels and they exhibit good stability and portability. The high specific surface area and increased porosity of nanostructures are favourable for the adsorption and diffusion of analytes.[18] To examine the efficiency of the xerogel films in CO_2 gas detection, xerogel films were fabricated on a quartz support by following a drop-casting procedure using a solution of **1** in toluene.

SEM and TEM analyses of the xerogel films obtained from evaporation (Fig. S13, ESI†) show a dense 3D network made of fibers of several micrometers in length. The xerogel film initially emitted blue fluorescence, with a maximum at 460 nm (Fig. 4a, inset), which was blue-shifted relative to the corresponding gel having an emission maximum at 465 nm. This xerogel film was sealed in a quartz vial in the presence of DEA vapor (Fig. S14, ESI†) and known volumes of CO_2 were added while monitoring the emission. As can be seen in Fig. 4a, the emission intensity gradually decreased and slightly blue shifted in the 0–6000 ppm range. A linear calibration line (R = 0.9953) was attained over the range of 0 ppm to 2000 ppm (Fig. 4b) and from that, the detection limit of the xerogel film was calculated to be as low as 4.5 ppm. This figure, if compared with the one previously determined for the gel aggregate system, represents a significant improvement, of more than two orders of magnitude (compare 4.5 to 908 ppm). Interestingly, we also noticed that if the xerogel film, after being exposed to different quantities of CO_2, was removed from the cuvette and completely dried, its emission exhibited a distinct modulation (Fig. 5a). Indeed, the solid residue showed a change of emission from blue to green depending on the quantity of CO_2 present (Fig. 5b). In particular, as evidenced by the spectrum in Fig. 5a (red line), green emission results from the appearance of a new emission band at *ca.* 550 nm. The same behaviour can be observed by the addition of (TBA)Cl to the xerogel (Fig. S15, ESI†), but also it could be observed with the gel aggregate samples after CO_2 exposure and solvent evaporation (Fig. S16, ESI†). This highlights the role of the anion–gelator HB complex in modulating the emission of the material.

A further confirmation of the actual formation of the HB complex is given by ^{1}H-NMR analysis of the xerogel sensor materials after use and being dried, which, when dissolved in DMSO-d_6, produce spectra where the typical HB downfield shifts are present for the Ha and Hc signals of **1** (Fig. 5c), fully consistent with what was observed in the previously described titration experiments.

These findings represent the basis for an improved CO_2 sensor system based on xerogels of **1**-toluene, which is based on two features. First, the xerogel films, made from evaporation of supramolecular gels, possess an equal and smooth spatial distribution and large surface area,[19] which efficiently promotes the attainment of a low detection limit. Secondly, the xerogel film system works in a dual mode, as both emission quenching and emission modulation can be used to determine CO_2 concentration. This latter modality, although working only for a high

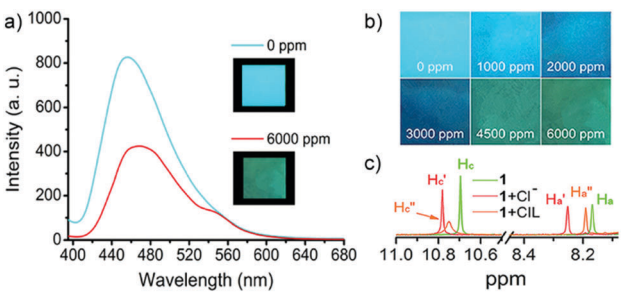

Fig. 5 (a) Fluorescence spectra of the xerogel films exposed to different CO_2 concentrations after drying; (b) images under illumination at 365 nm of the xerogel films exposed to different CO_2 concentrations after drying; (c) ^{1}H-NMR spectra in DMSO-d_6 of the xerogel sample, as is and after addition of CIL and (TBA)Cl and drying.

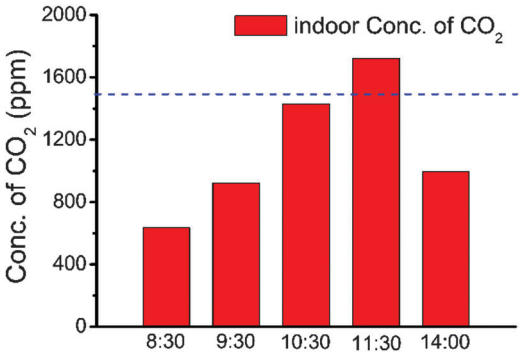

Fig. 6 Concentration changes of indoor CO_2 concentration (ppm) in a student classroom (8 : 30 – 11 : 30) and after ventilation when teaching was over (14 : 00). Dashed line = 1500 ppm, recommended level.

CO_2 concentration (>4000 ppm), can allow for sensing of CO_2 by the naked eye, just by illuminating the solid sensor under UV-light (λ_{ex} = 365 nm). The response to CO_2 is also highly selective among other gases present in the atmosphere (O_2, N_2, Ar) and CH_4 (see Fig. S17, ESI†). However, a significant interference is found with SO_2 and NO_2 even if present at a concentration as low as 1%.[20]

Finally, we report on the use of the above described xerogel based sensor for the detection of CO_2 in real case scenarios, *i.e.*, one of our laboratory facilities and a student classroom. We put the xerogel film sensor system in contact with the atmosphere of a busy laboratory and we monitored the emission. As expected, the band centered at 460 nm decreased in intensity and, after *ca.* 100 seconds, no further change in emission was observed (Fig. S18, ESI†). By making use of the calibration line previously obtained, the concentration of CO_2 within the laboratory was calculated as 683 ppm, a value that can be explained by the presence of several actively working collaborators in the room, but below the threshold usually set as a limit for safety reasons. Following the same methods, the CO_2 concentration of a crowded room where students are having classes was monitored by the same sensor apparatus. As can be seen from Fig. 6 and Fig. S19 (ESI†), the indoor CO_2 concentration rose with time and it exceeded the recommendation level of 1500 ppm given by the Finnish Housing Health Guidelines.[21]

In order to check the validity of these CO_2 concentration measurements, we also compared the performance of our xerogel system with that of a commercial CO_2 detector. We thus prepared three air samples at known CO_2 concentrations (500, 1000 and 1600 ppm) and compared the detector readings with the CO_2 value determined with our xerogel sensor. A very good agreement was found (see Fig. S20, ESI†), thus validating the system's potential for real-world application.

Conclusions

In conclusion, we have designed novel fluorescent sensor systems for CO_2 based on gel aggregates and xerogel films made of an AIE bis-cyanostilbene derivative, **1**, whose properties were studied in detail by a combination of several techniques, ^{1}H-NMR spectroscopy, FT-IR spectroscopy, DLS, electron microscopy and fluorescence spectroscopy. The working principle of our sensor systems relies on the HB driven recognition of the CIL anion, formed *in situ* by the reaction of CO_2 with DEA. The carbamate anion of CIL binds to gelator **1** affecting its aggregation state and consequently its emission. As far as the gel aggregate system is concerned, a gel to solution transformation along with emission quenching can be obtained by adding CO_2 into a dispersion of micrometer-sized gel aggregates of **1** in toluene in the presence of a controlled excess of DEA. The fluorescence signal can be used to sense CO_2 with a detection limit of 908 ppm. This sensitivity can also be tremendously improved to 4.5 ppm by replacing the above-mentioned gel aggregates in solution with xerogel films of **1** drop-casted onto a quartz template and exposed to DEA vapor. Furthermore, this second sensor setup, which has been validated by comparison with a commercial NDIR detector (see ESI†), can work in a dual mode, both by emission quenching and emission modulation. The CO_2 response can be detected by the naked eye, provided illumination of the solid sensor material by 365 nm light is applied, but only if the concentration of CO_2 is high (>4000 ppm). The sensor systems reported here, at variance with other systems described in the literature, rely on a HB-driven host–guest complex formation and they are promising for the construction of xerogel-based devices for the detection of CO_2 in real-world applications.

Conflicts of interest

There are no conflicts to declare.

Acknowledgements

This work was supported by the National Natural Science Foundation of China (51673082 and 21374036), a Croatian-Chinese bilateral project and in part by the Croatian Science Foundation under the project IP-2016-06-5983.

Notes and references

1 (*a*) R. Monastersky, *Nature*, 2013, **497**, 13–14; (*b*) R. S. Haszeldine, *Science*, 2009, **325**, 1647–1652.

2 (*a*) O. S. Wolfbeis, B. Kovacs, K. Goswami and S. M. Klainer, *Microchim. Acta*, 1998, **129**, 181–188; (*b*) R. Pierantozzi in *Encyclopedia of Chemical Technology*, ed. J. I. Kroschowitz, Wiley, New York, 4th edn, 1991, vol. 4, pp. 803–822; (*c*) D. Leaf, H. J. H. Verolme and W. F. Hunt, Jr., *Environ. Int.*, 2003, **29**, 303–310.

3 L. de Lary, A. Loschetter, O. Bouc, J. Rohmer and C. M. Oldenburg, *Int. J. Greenhouse Gas Control*, 2012, **9**, 322–333.

4 (*a*) R. N. Dansby-Sparks, J. Jin, S. J. Mechery, U. Sampathkumaran, T. W. Owen, B. D. Yu, K. Goswami, K. L. Hong, J. Grant and Z. L. Xue, *Anal. Chem.*, 2010, **82**, 593–600; (*b*) S. Neethirajan, D. S. Jayas and S. Sadistap, *Food Bioprocess Technol.*, 2009, **2**, 115–121; (*c*) G. Eranna, B. C. Joshi, D. P. Runthala and R. P. Gupta, *Crit. Rev. Solid*

State Mater. Sci., 2004, **29**, 111–188; (*d*) Y. Amao and N. Nakamura, *Sens. Actuators, B*, 2005, **107**, 861–865; (*e*) O. Oter, K. Ertekin and S. Derinkuyu, *Talanta*, 2008, **76**, 557–563; (*f*) C. S. Chu and Y. L. Lo, *Sens. Actuators, B*, 2008, **129**, 120–125.

5 (*a*) M. Vendrell, D. Zhai, J. C. Er and Y. Chang, *Chem. Rev.*, 2012, **112**, 4391–4420; (*b*) X. Zhou, S. Lee, Z. Xu and J. Yoon, *Chem. Rev.*, 2015, **115**, 7944–8000; (*c*) Z. Guo, N. R. Song, J. H. Moon, M. Kim, E. J. Jun, J. Choi, J. Y. Lee, C. W. Bielawski, J. L. Sessler and J. Yoon, *J. Am. Chem. Soc.*, 2012, **134**, 17846–17849; (*d*) Q. Xu, S. Lee, Y. Cho, M. H. Kim, J. Bouffard and J. Yoon, *J. Am. Chem. Soc.*, 2013, **135**, 17751–17754.

6 (*a*) Y. Hong, J. W. Y. Lam and B. Z. Tang, *Chem. Soc. Rev.*, 2011, **40**, 5361–5388; (*b*) J. Mei, Y. Hong, J. W. Y. Lam, A. Qin, Y. Tang and B. Z. Tang, *Adv. Mater.*, 2014, **26**, 5429–5479; (*c*) R. T. K. Kwok, C. W. T. Leung, J. W. Y. Lam and B. Z. Tang, *Chem. Soc. Rev.*, 2015, **44**, 4228–4238.

7 (*a*) Y. Ma, H. Xu, Y. Zeng, C. Ho, C. Chui, Q. Zhao, W. Huang and W. Wong, *J. Mater. Chem. C*, 2015, **3**, 66–72; (*b*) R. Ali, S. S. Razi, R. C. Gupta, S. K. Dwivedi and A. Misra, *New J. Chem.*, 2016, **40**, 162–170; (*c*) G. Xia, Y. Liu, B. Ye, J. Sun and H. Wang, *Chem. Commun.*, 2015, **51**, 13802–13805; (*d*) M. Ishida, P. Kim, J. Choi, J. Yoon, D. Kim and J. L. Sessler, *Chem. Commun.*, 2013, **49**, 6950–6952.

8 (*a*) S. Pandey, S. N. Baker, S. Pandey and G. A. Baker, *Chem. Commun.*, 2012, **48**, 7043–7045; (*b*) Y. Liu, Y. Tang, N. N. Barashkov, I. S. Irgibaeva, J. W. Y. Lam, R. Hu, D. Birimzhanova, Y. Yu and B. Z. Tang, *J. Am. Chem. Soc.*, 2010, **132**, 13951–13953; (*c*) H. Wang, D. Chen, Y. Zhang, P. Liu, J. Shi, X. Feng, B. Tong and Y. Dong, *J. Mater. Chem. C*, 2015, **3**, 7621–7626.

9 (*a*) J. K. Gupta, D. J. Adams and N. G. Berry, *Chem. Sci.*, 2016, **7**, 4713–4719; (*b*) J. Raeburn and D. J. Adams, *Chem. Commun.*, 2015, **51**, 5170–5180; (*c*) Y. Lan, M. G. Corradini, R. G. Weiss, S. R. Raghavan and M. A. Rogers, *Chem. Soc. Rev.*, 2015, **44**, 6035–6058; (*d*) S. Datta and S. Bhattacharya, *Chem. Soc. Rev.*, 2015, **44**, 5596–5637.

10 (*a*) J. Jiang, G. Ouyang, L. Zhang and M. Liu, *Chem. – Eur. J.*, 2017, **23**, 9439–9450; (*b*) D. B. Amabilino, D. K. Smith and J. W. Steed, *Chem. Soc. Rev.*, 2017, **46**, 2404–2420; (*c*) H. Shigemitsu and I. Hamachi, *Acc. Chem. Res.*, 2017, **50**, 740–750; (*d*) C. D. Jones and J. W. Steed, *Chem. Soc. Rev.*, 2016, **45**, 6546–6596; (*e*) M. Cametti and Z. Džolić, *Chem. Commun.*, 2014, **50**, 8273–8286.

11 (*a*) Y. Zhang, Y. Ma, M. Deng, H. Shang, C. Liang and S. Jiang, *Soft Matter*, 2015, **11**, 5095–5100; (*b*) Y. Zhang, C. Liang, H. Shang, Y. Ma and S. Jiang, *J. Mater. Chem. C*, 2013, **1**, 4472–4480; (*c*) Y. Zhang and S. Jiang, *Org. Biomol. Chem.*, 2012, **10**, 6973–6979.

12 Y. Ma, M. Cametti, Z. Džolić and S. Jiang, *J. Mater. Chem. C*, 2016, **4**, 10786–10790.

13 (*a*) B. An, S. Kwon, S. Jung and S. Y. Park, *J. Am. Chem. Soc.*, 2002, **124**, 14410–14415; (*b*) P. Xing, H. Chen, L. Bai and Y. Zhao, *Chem. Commun.*, 2015, **51**, 9309–9312.

14 (*a*) J. Luo, Z. Xie, J. W. Y. Lam, L. Cheng, H. Chen, C. Qiu, H. S. Kwok, W. Zhan, Y. Liu, D. Zhu and B. Z. Tang, *Chem. Commun.*, 2001, 1740–1741; (*b*) M. Levitus, K. Schmieder, H. Ricks, K. D. Shimizu, U. H. F. Bunz and M. A. Garcia-Garibay, *J. Am. Chem. Soc.*, 2001, **123**, 4259–4265.

15 More detailedly, the solution state is achieved with ca. 1 equivalent of (TBA)Cl and (TBA)Br, 1.5 equivalents of (TBA)OAc and ca. 4 equivalents of CIL. No effect was observed with other anions such as (TBA)PF6, (TBA)ClO_4 and (TBA)I, while (TBA)NO_3 can destroy the gel, but only after addition of ca. 10 equivalents.

16 DMSO is a commonly used polar aprotic solvent for anion binding studies and **1** does not form gel in it. Notably, we had to add water as a co-solvent in order to increase the rate by which association occurs in order to be able to run titration experiments.

17 A qualitatively similar behaviour was found for other ions, see Fig. S5 ESI†.

18 (*a*) J. Peng, J. Sun, P. Gong, P. Xue, Z. Zhang, G. Zhang and R. Lu, *Chem. – Asian J.*, 2015, **10**, 1717–1724; (*b*) X. Qian, W. Gong, M. K. Dhinakaran, P. Gao, D. Na and G. Ning, *Soft Matter*, 2015, **11**, 9179–9187.

19 (*a*) R. Miao, J. Peng and Y. Fang, *Mol. Syst. Des. Eng.*, 2016, **1**, 242–257; (*b*) R. Miao, J. Peng and Y. Fang, *Langmuir*, 2017, 10419–10428.

20 (*a*) W. Wu, B. Han, H. Gao, Z. Liu, T. Jiang and J. Huang, *Angew. Chem., Int. Ed.*, 2004, **43**, 2415–2417; (*b*) G. Yuan, F. Zhang, J. Geng and Y. Wu, *RSC Adv.*, 2014, **4**, 39572–39575.

21 T. Vehvilainen, H. Lindholm, H. Rintamaki, R. Paakkonen, A. Hirvonen, O. Niemi and J. Vinha, *J. Occup. Environ. Hyg.*, 2016, **13**, 19–29.